SCIENCE CHINA
Earth Sciences

• RESEARCH PAPER •

October 2016 Vol.59 No.10: 2053–2061
doi: 10.1007/s11430-016-0015-6

Dust levitation and transport over the surface of the Moon

LI Lei[1*], ZHANG YiTeng[1,2], ZHOU Bin[1] & FENG YongYong[1]

[1] *State Key Laboratory of Space Weather, National Space Science Center, Chinese Academy of Sciences, Beijing 100190, China;*
[2] *University of Chinese Academy of Sciences, Beijing 100190, China*

Received January 20, 2016; accepted May 18, 2016; published online August 30, 2016

Abstract Exposed to space plasma and solar radiation, electrostatic potential may build up in the lunar regolith, leading to a wealth of dust phenomena, including levitation, oscillation, and transport over the surface. Based on plasma sheath theory, the global near-surface plasma environment is modeled, and the dynamics of charged dust are investigated. Results show that sub-micron sized dust particles can be levitated by the electric field over the surface, forming a dust belt that changes in position and thickness depending on the solar zenith angle. On the dayside of the Moon, stably levitated particles are about ten times smaller, and collect in a thinner belt closer to the surface than do those on the nightside. Although the size and charge of stably levitated dust particles are dependent on ambient plasma conditions, initial charge and velocity, which are closely related to the dynamics of dust particles including charging, oscillation, and damping, will determine whether, or not, a particle can attain stable levitation. Horizontal electrostatic dust transport near to the terminator region may lead to net deposition of dust from the dark into the sunlit hemisphere. Finally, because of different charging processes that result due to rotation of the Moon, before precipitation, dust particles in the dusk terminator region may be transported much longer distances and oscillate to much higher altitude than these in the dawn terminator.

Keywords Moon, Lunar dust, Dust particle dynamics, Electrostatic levitation

Citation: Li L, Zhang Y T, Zhou B, Feng Y Y. 2016. Dust levitation and transport over the surface of the Moon. Science China Earth Sciences, 59: 2053–2061, doi: 10.1007/s11430-016-0015-6

1. Introduction

As the Moon has no significant atmosphere, the lunar surface is exposed to the full impact of solar radiation and plasma, which results in photoelectron emissions and plasma charging. As a result, a plasma sheath develops above the lunar surface, containing an electric field that varies with respect to incoming solar radiation and space plasma (Manka, 1973).

The lunar surface is covered by regolith, or lunar soil, mostly comprising small particles with a wide variation in size. Of these, particles smaller than 100 μm in size are usually called lunar dust. Analysis of lunar samples indicates about 20 weight percentage of the regolith comprises particles that are smaller than 20 μm (Colwell et al., 2007), with an even smaller fraction made up of sub-micron, even nanometer-sized, particles. These dust particles are subject to the same charging mechanisms as the lunar surface; actually, since this dust is dielectric, it is prone to accumulating charge. If the lunar surface sheath electrostatic force on a charged dust particle is larger than the sum of gravity and cohesion between the dust and the surface, the particle will be levitated and transported.

Ubiquitous dust in the lunar environment was noticed by the first Apollo astronauts; subsequently, several Surveyor spacecraft have observed 'horizon glow' 10−30 cm in vertical extent above the western horizon of the Moon after local sunset, probably due to light scattered by levitated dust particles (Rennilson and Criswell, 1974). On the lunar surface, the Lunar Ejecta and Meteorites (LEAM) Experiment

* Corresponding author (email: lil@nssc.ac.cn)

of Apollo 17 detected slow moving, highly charged, dust particles in larger numbers before sunset, which suggests they are launched on long trajectories from the terminator region (Berg et al., 1976). More recently, the Clementine spacecraft also detected high-altitude lunar horizon glow, which might also be attributable to lunar dust (Zook et al., 1995). Since lunar dust has cohesive characteristics, it could potentially have severe and harmful effects on lunar surface missions. Thus, in order to explain these observed phenomena, and to effectively implement mitigating strategies, a number of theoretical approaches have been applied to investigate the charging, levitation, and transport of dust particles.

Suppose that dust particles have the same charge, if $\left|\frac{Qn_d}{en_0}\right| \ll 1$, where n_0 and n_d are the ambient plasma and dust particle number density, respectively, then modifications caused by charged dust particles to the sheath potential and plasma profiles would be negligible. In this case, the sheath is referred to as "tenuous" (Nitter et al., 1994). A good deal of research has been conducted on this tenuous sheath, determining the electric field and plasma using a sheath model that enables the charging and dynamic processes of dust to be traced. In this way, basic properties of dust particle dynamics, including oscillation, damping, stability, and trapping, can be investigated (e.g., Nitter and Havnes, 1992; Colwell et al., 2005).

The terminator region on the Moon is the place where surface potential switches from positive to negative (Freeman and Ibrahim, 1975). Horizontal electric field is thought to exist in the terminator region, which would function to launch dust particles over long distances. However, due to a lack of observational data, uncertainties remain about the nature of the plasma environment that extends from the terminator region deep into the lunar wake. To date, observations and research on the lunar sheath and dust dynamics have been limited in most cases to the dayside, and in particular have focused on the subsolar region (Nitter et al., 1998; Poppe and Horányi, 2010). As a result, quantitative estimates of the global properties of the lunar sheath and dust dynamics are currently lacking.

In this paper, we present a global lunar sheath model that has been developed on the basis of lunar plasma observations over recent years (i.e., Halekas et al., 2005; Nishino et al., 2009a, 2009b). Using this model, we investigate the basic features of dust particle dynamics at different solar zenith angles (sza), as well as their transport near the terminator region.

2. Methods

2.1 Sheath and electric field

Submerged in solar plasma and exposed to solar radiation, the Moon has a surface potential that builds up on its surface. Responsible for this, collection of solar wind electrons, ions, and solar UV induced photoemission are thought to be the most important charging currents, although electrons in the lunar wake with relatively high energies may also induce some secondary electron emissions (Whipple, 1981).

As the Debye length (λ_D) is much smaller than the lunar radius (R_m), and ignoring local geologic features, the thin sheath can be described using a one-dimensional model (Guernsey and Fu, 1970), in which charged particle densities are correlated with the sheath potential via Poisson's equation, as follows:

$$\nabla^2 V = -\frac{e}{\varepsilon_0}(n_i - n_e - n_p), \tag{1}$$

where V is the potential, n_i and n_e are the number densities of incoming solar wind protons and electrons, n_p is the number density of photoelectrons emitted by the lunar surface under the impact of solar UV, e is the electron charge, and ε_0 is the vacuum permittivity.

Thus, every particle species inside the sheath has its velocity v, and electric potential energy, governed by the energy conservation equation:

$$\frac{1}{2}mv^2 - eV = \frac{1}{2}mv_0^2 - eV_0, \tag{2}$$

In this relationship, the subscript "0" denotes the initial state, unperturbed solar wind ion/electron, or photoelectron newly emitted by the surface.

It is assumed that incoming solar wind electrons, and photoelectrons emitted from the lunar surface, have Maxwellian velocity distributions, as follows:

$$f_j(x,v) = n_j\left(\frac{m_e}{2\pi kT_j}\right)^{3/2}\exp\left(-\frac{m_e v^2}{2kT_j} + \frac{e(V(x)-V_0)}{kT_j}\right), \tag{3a}$$

where m_e is electron mass, n_j is number density, T_j is electron temperature, k is Boltzmann's constant, j=e for solar wind electrons, and j=p for photoelectrons emitted by the lunar surface. In this model, solar wind ions are considered to be cold with just a drifting velocity, which can be related to their unperturbed condition using the mass conservation equation:

$$n_i v = n_{i0} v_0. \tag{3b}$$

With plasma quasi-neutrality and zero net current conditions at infinity, solving eqs. (1)–(3) enables calculation of the potential and particle density profiles inside the sheath (Nitter et al., 1998).

Further, assuming nominal solar wind conditions in the lunar orbit, that is a solar wind with a density of 5 cm^{-3}, and taking a velocity of 350 km/s, an electron temperature of 15 eV, and electron density and temperature measurements taken by Lunar Prospector from the lunar plasma wake (Halekas et al., 2005), it is possible to determine sheath profiles at different sza values (Figure 1).

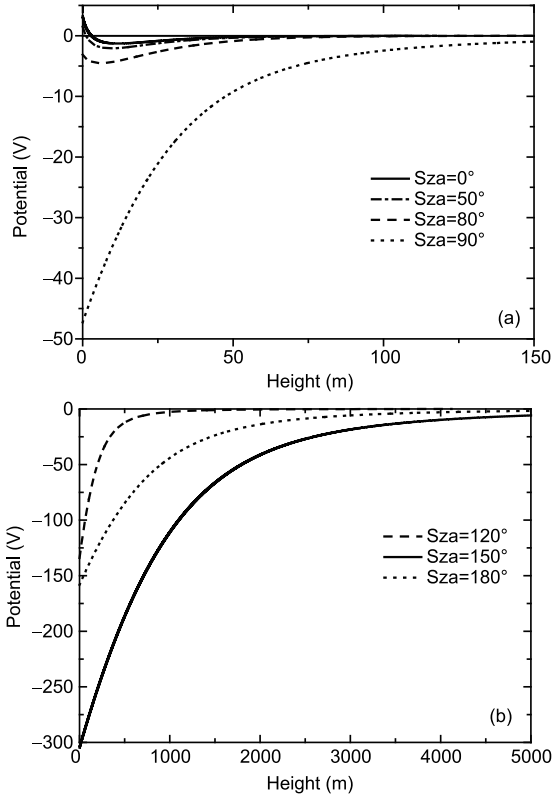

Figure 1 Sheath potential profiles for different sza values. (a) Dayside and terminator region; (b) nightside.

Calculations show that the sheath exhibits a non-monotonic profile in most regions at dayside (Figure 1). Furthermore, the dayside sheath is usually thin, which implies that the near-surface electric field resulting from surface charging is confined to a layer close to the surface. In contrast, the nightside sheath can extend several kilometers, and the associated vertical electric field can remain strong high above the surface. These differences in profiles at different sza values imply that a horizontal electric field may exist near the lunar surface, especially at sza values of more than 80°.

Thus, based on one-dimensional sheath profiles, we attempt to determine the nature of the electric field in the lunar spherical coordinate system by differentiating the potential horizontally and vertically. Figure 2 shows the surface radial (a), and longitudinal (b), components of the electric field as a function of longitude (ϕ) and colatitude (θ). Since the potential profile is sza dependent, and we ignore the aberration of the solar wind, the electric field is symmetric about the subsolar point. It is also clear that the radial component (E_r) is largest at the subsolar point, trending to zero at about a sza of 86°, before becoming negative and reaching a minimum at a sza of about 90°. The longitudinal component (E_ϕ) is much weaker than the radial one; at dayside, the longitudinal component is negligible when sza is less than 60°, but becomes significant near the dawn and dusk terminator regions. At the equator of the dusk hemisphere (i.e., ϕ>0), the longitudinal component

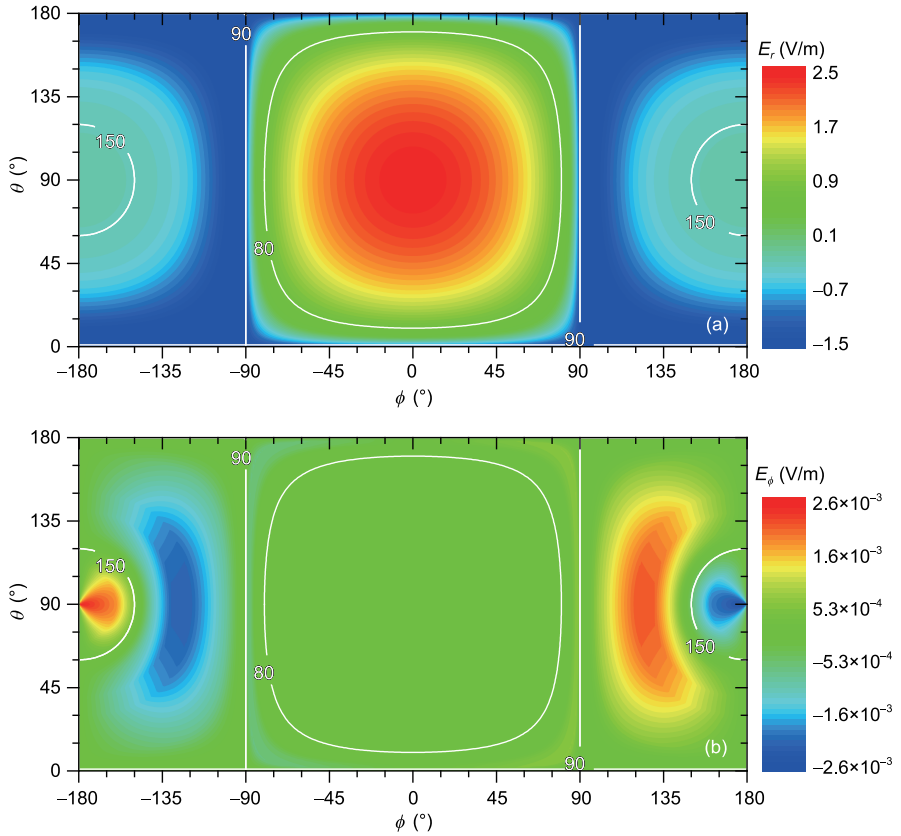

Figure 2 Electric field on the lunar surface, with sza shown by white lines. (a) Radial component; (b) longitudinal component.

points to local east if ϕ is less than 150°, or shifts to the west if ϕ is greater than 150°, as the electron temperature reaches a maximum when ϕ is equal to 150° (Halekas et al., 2005). There is a small increase in E_ϕ near to the terminator region (sza=90°), as solar flux is proportional to cos(sza), resulting in significant differential charging when sza is greater than approximately 80°. However, when sza is greater than 90°, there is no solar radiation and just a flat solar wind electron distribution, differential charging almost disappears. When solar wind parameters begin to change via sza in the lunar wake, E_ϕ increases again.

2.2 Dust particle dynamics

Dust particles are subject to the same charging mechanisms as the lunar surface. However, because the radius of a dust particle, r_d, is usually much less than the Debye length in the lunar surface plasma environment (i.e., $r_d \ll \lambda_D$), it is assumed that these particles remain tenuous in the sheath (i.e. $r_d \ll d$), and electrically isolated from one another. Dust particle charge, Q, can be approximated using vacuum capacitance, $Q = 4\pi\varepsilon_0 aU$, where U is the dust particle potential relative to the local plasma potential, V. The forces acting on a charged dust particle include electromagnetic, gravitational, and Coulomb forces from the sheath plasma, as well as neutral drag from the lunar exosphere. However, because either the solar wind or the lunar exosphere is tenuous, neutral drag, or Coulomb force, can be neglected. Moreover, because the Lorentz force acting on the slowly moving dust due to solar wind magnetic field is much smaller than electrostatic force, the balance between electric force and gravity determines the motion of the dust particle.

The transport of a dust particle can be simulated in a frame fixed on the surface of the Moon, originating at the initial position of the dust particle (θ, ϕ), with x pointing to the east, y pointing to the north, and z pointing to the sky, perpendicular to the lunar surface. Thus, the equations of motion and charging for a dust particle can be written as follows:

$$\begin{cases} m\dfrac{\mathrm{d}v_x}{\mathrm{d}t} - \left(2\Omega\sin\theta + \dfrac{v_x\tan\theta}{R_\mathrm{m}}\right)v_y + \dfrac{v_z}{R_\mathrm{m}}v_x \\ \qquad + v_z\cdot 2\Omega\cos\theta = Q(t)E_x, \\ m\dfrac{\mathrm{d}v_y}{\mathrm{d}t} + \left(2\Omega\sin\theta + \dfrac{v_x\tan\theta}{R_\mathrm{m}}\right)v_x + \dfrac{v_z}{R_\mathrm{m}}v_y = Q(t)E_y, \\ m\dfrac{\mathrm{d}v_z}{\mathrm{d}t} - \dfrac{v_x^2+v_y^2}{R_\mathrm{m}} - v_x\cdot 2\Omega\cos\theta = Q(t)E_z - m\mathrm{g}, \end{cases} \tag{4}$$

$$\frac{\mathrm{d}\mathbf{x}}{\mathrm{d}t} = \mathbf{v}, \tag{5}$$

$$\frac{\mathrm{d}Q}{\mathrm{d}t} = I. \tag{6}$$

In these relationships, m is dust particle mass, x is position, v (v_x, v_y, v_z) is particle velocity, and Q is dust particle charge, time dependent because the charging current, I, varies as the particle moves to different positions. In addition, $\mathrm{R_m}$ is the average radius of the Moon (1737 km), g is acceleration due to gravity (1.62 m $\mathrm{s^{-2}}$ at the Moon), and Ω is the angular velocity of the Moon (2.66×10^{-6} rad $\mathrm{s^{-1}}$). Note that in eq. (4), terms involving Ω are Coriolis terms, while terms involving $1/R_\mathrm{m}$ result from consideration of the curvature of the Moon. Usually, if the velocity of particles is not very high, these two terms are small compared with gravity, or electric force, especially in the vertical direction where gravity and vertical electric forces dominate.

During the motion of a dust particle, all charged particles it encounters can contribute to the charging current. Thus, the charging currents from electrons can be obtained by integrating the distribution function in eq. (3) over velocity space, as follows:

$$I_j = -\mathrm{e}\iint_v\int v\sigma_e f_j(x,v)\mathrm{d}v, \tag{7}$$

where $j=e$ for solar wind electrons, and $j=p$ for photoelectrons emitted by the lunar surface. Note that σ_e is the electron collision cross section, $\sigma_e = \pi a^2(1+2\mathrm{e}U/(\mathrm{m}_e v^2))$, $\mathrm{m_e}$ is electron mass, a is dust particle radius, and U is dust potential relative to the local plasma.

The solar wind ion current is given as follows:

$$I_i = \mathrm{e}n_0 v_0 \sigma_i, \tag{8}$$

where n_0 and v_0 are incoming solar wind density and velocity, respectively, $\sigma_i = \pi a^2[1-2\mathrm{e}U/(\mathrm{m}_i v_0^2 - 2\mathrm{e}V)]$ is ion collision cross section, and m_i is proton mass.

When collecting charge from the environment, the dust particle also emits photoelectrons when lit by the Sun:

$$I_d = \begin{cases} \pi {r_d}^2 J_d & U \le 0 \\ \pi {r_d}^2 J_d \exp(-\mathrm{e}U/\mathrm{k}T_{pe}) & U \ge 0 \end{cases}, \tag{9}$$

where J_d is the current density emitted by the dust particle, and T_{pe} is the emitted photon electron temperature, set here to values as defined by the experiment (i.e., J_d=4.5×10^{-6} A m^{-2}, and T_{pe}=1.47 eV; Willis et al., 1973).

Thus, the net current transferred to a dust particle is as follows:

$$I = I_i + I_e + I_p + I_d. \tag{10}$$

According to eq. (3), Q varies at a rate defined by I. However, because values for I depend on local plasma density, unless a grain is immobile for a long time, it cannot reach charge equilibrium, which means that the net current transferred will be zero.

In sum, within a pre-defined sheath (see above, section 2.1), and using eqs. (4)–(6) and the fourth-order Runga-Kutta method, it is possible to trace the motion, and charging processes, of a dust particle, and investigate its dynamics in a three-dimensional frame.

3. Results

3.1 Dust particle levitation

In the first place, we consider a case at the subsolar point (i.e., θ=90°, ϕ=0°), and assume that a spherical-shaped dust particle has a radius of 0.05 μm, a mass density of 1000 kg m^{-3}, an initial charge of 10e, and an initial velocity of 0.

Ignoring cohesion of the particle to the surface, as shown in Figure 3a where particle vertical position z (black line) and charge Q (red line) are illustrated as functions of time, the dust particle leaves the surface and passes into the sheath, as electric force can overcome the force of gravity. Data show that the particle accelerates upwards when the electric force is larger than gravity, and decelerates when the sheath electric field drops at high altitudes.

During this motion, currents change as shown in Figure 3b; in this graph, all currents are shown as absolute values in order to use the log scale (actually I_e and I_p are negative). The sheath photoelectron changes are most violent near the surface (sharp peak in Figure 3b), as the photoelectron density has the largest gradient in this position. In contrast, solar wind electron current varies in a smoother manner, with a tendency opposite to the photoelectron current, while the current emitted by the dust particle declines exponentially as its potential, U, increases. Figure 3b also shows that the solar wind ion current does not change, since the positive dust potential does not significantly retard incoming ions with high drift velocities. Throughout this process, except at early stages when particles stay near the surface where photoelectron density is high, the dust particle emission current dominates over all others, and the charge on the particle increases. Gradually, the dust particle position converges towards a certain height but total charge continues to increase at t=1000 s. Actually, data show that in fact it takes more than 1 hour for a dust particle to reach its equilibrium potential, as charging currents in the lunar sheath are very low. Finally, the dust emission current added to the incoming ion current acts to almost balance environmental electron currents.

During a simulation lasting 1000 s, horizontal displacement of the dust particle is less than 0.1 m, which means that the horizontal electric field component is negligible in the subsolar region. In addition, because sza changes by about 0.15°, solar flux change is also negligible.

Since the horizontal electric field is negligible in the subsolar region, and the velocity of the dust particle is low, eq. (4) can be reduced to a momentum equation in the vertical direction, as follows:

$$m\frac{\mathrm{d}v_z}{dt} = QE_z - m\mathrm{g} = F. \tag{11}$$

Thus, integration of eq. (11) results in an energy equation for the dust particle:

$$\frac{v_{z,2}^2}{2} + \frac{Q_2V_2}{m} + \mathrm{g}z_2 = \frac{v_{z,1}^2}{2} + \frac{Q_1V_1}{m} + gz_1 + \int_{t_1}^{t_2}\frac{IV}{m}\mathrm{d}t. \tag{12}$$

In this expression, the fourth term on the right represents the energy created by the charging currents. Without this fourth term, eq. (12) resembles an ordinary energy conservation equation in the potential fields, and the velocity of the particle is just the function of position. Thus, inclusion of the fourth term in eq. (12) changes the charge balance and also introduces non-linear effects into the system. According to eq. (11), as the grain charge increases, the force equilibrium position (F=0) becomes higher. In the sheath when sza is zero (Figure 1), the fourth term in eq. (12) is usually negative when the dust particle accumulates positive charge (I > 0). This means the particle will lose energy, resulting in damped oscillations (Figure 3).

Stable levitation is established at a height where both charge and force are in equilibrium, or I=0 and F=0 (Nitter et al., 1998). Thus, when I=0, we can determine the equilibrium dust particle potential, U_{eq}, as a function of height (dashed line in Figure 4). Results show that at high altitudes where photoemission dominates, U_{eq} is close to the value of photoelectron energy, T_{pe}, in eV. Indeed, as total charge (and hence electric force) is determined by U_{eq} and the capacitance of

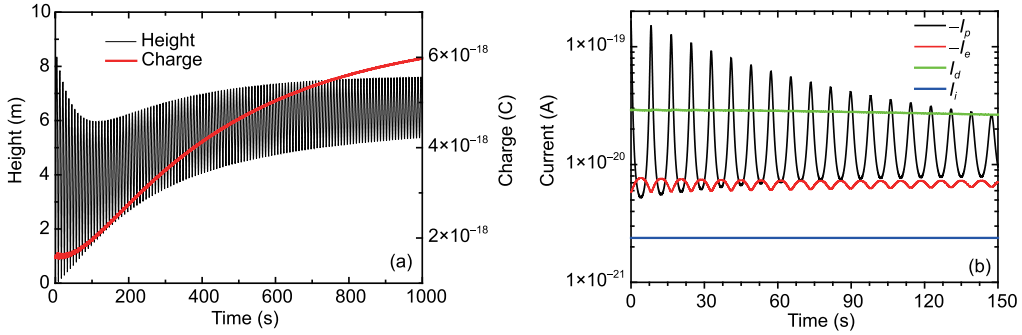

Figure 3 Dust particle levitation when sza=0, r_d=0.05 μm, v_{z0}=0, and Q_0=7e. (a) Vertical position (black line) and charge (red); (b) absolute charging current values from photoelectrons in the sheath (black), solar wind electrons (red), solar wind ions (black), and dust emitted photoelectrons (green).

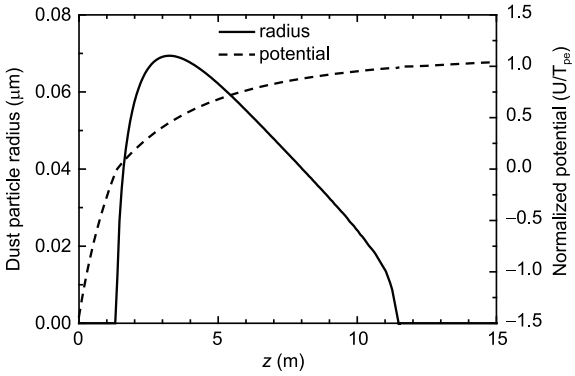

Figure 4 Radius of the levitated dust particle, and equilibrium dust potential as functions of height, when sza is zero.

the dust particle, at certain altitudes, only particles of certain sizes (solid line in Figure 4) are able to attain a force balance (F=0), and thus suspend in the sheath. Results show that although there might be two force equilibrium positions for particles of a certain size (Figure 4). The position at higher altitude will be the stable one since it has minimum potential energy, according to eq. (12). It is also the case that stable levitation (i.e., height, charge) can only be determined by grain size under certain sheath profiles, irrespective of initial velocity or charge.

The solid curve in Figure 4 implies that force equilibrium is only possible in a belt above the surface. In the subsolar region, since the sheath has a non-monotonic potential profile (Figure 3), at heights more than about 10 m, the electric field turns downwards, and can no longer suspend positively charged dust particles. In contrast, at heights less than about 1 m, the sheath is dominated by photoelectrons, U_{eq} is negative, and no stable levitation is possible as the electric field points upwards. The levitation belt over the lunar surface is shown in Figure 5, which shows that dust can only be suspended within the belt bracketed by the grey lines. The levitation belt at dayside is usually thin, and close to the lunar surface; when the sza is higher than about 70°, the lower boundary of this belt drops to the surface, while at nightside, the belt is much thicker and higher, as the scale height of the sheath is much larger. The solid line (Figure 4) indicates the position at which the largest particle suspends; higher than this, particles can be levitated stably at a height inverse to their size, while levitation is unstable below this level. No stable levitation is possible in the shaded region near to the point where the sza is equal to 90° (Figure 5), and where U_{eq} is positive, because the dust particle will be fully sunlit, and the vertical electric field is negative.

Results also show (Figure 4) that there is a maximum particle radius that can be levitated; when the sza equals zero, and under nominal solar wind conditions, the maximum radius of levitated dust is less than 0.07 μm. As the sheath profile changes with sza, the maximum size of particle changes accordingly (dashed line in Figure 5); as sza increases, the surface potential decreases together with the vertical electric field (Figure 1a), and the size of dust particles that can be suspended by the electric field gets smaller. Indeed, when the sza is higher than about 70° (Figure 1a), the surface potential turns negative, the potential gradient and electric field in the sheath increase, and larger particles can be levitated. On the nightside of the Moon, negatively charged particles with radii almost ten times larger than on the dayside can be levitated.

As described above, stable levitation is only dependent on r_d and sza. However, initial charge and velocity may also be important to determine if it is feasible for a particle to reach final stable levitation.

A large initial charge with the same polarity as the surface potential means a large initial electric potential, which determines the initial amplitude of oscillation and charging cur-

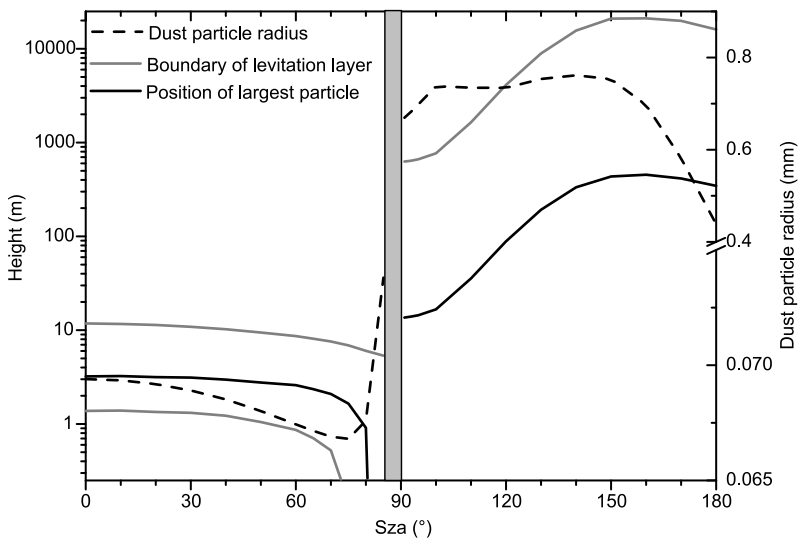

Figure 5 Dust levitation belt, and maximum radius of levitated particles, over the lunar surface.

rents during motion. Thus, as shown by eq. (12), too large an initial charge may reduce the photoelectron emission of the particle and enlarge the electron current from the environment. Also according to eq. (12), if net current, I, is always negative, the energy of the particle will increase, resulting in amplified oscillation, which may deposit the particle into the regolith. However, if there is a suitable initial charge, $I\times V$ remains negative, and a particle will have damped oscillation; except at a very early stage, when the particle moves near the surface where photoelectron density is high, the charge will increase, and the trajectory will move higher to the stable levitation height (Figure 3). However, if the initial charge drops from 10e to 7e, with low initial electric potential energy, the particle oscillates longer in the region where the photoelectron density is high, I and $I\times V$ are both negative, the particle loses both charge and energy. Subsequently, the trajectory lowers to the unstable levitation height, and finally oscillation stops (Figure 6).

Initial speed, v_{z0}, is not really relevant for a particle to reach stable levitation. This is because, as mentioned above, for an ordinary energy conservation system in potential fields, particle speed is just a function of position; a particle will have the same speed when it oscillates back to the surface, and will be caught in the regolith. A difference is due to the fourth term on the right-hand side in eq. (12): some kinetic energy may be converted to extra electric potential energy due to charge loss, or gain. If the kinetic energy is totally converted to potential energy when the particle oscillates back to the surface, the following relationship follows:

$$\frac{(q-q_0)}{m}V_0=\frac{v_{z0}^2}{2}+\int_0^t\frac{IV}{m}\mathrm{d}t. \tag{13}$$

However, in just one period of oscillation, charge change and energy loss are small due to the low charging currents in the lunar sheath, which means that if v_{z0} is large, the equation above becomes irrelevant, and the particle will fall into the regolith at high speed. In other words, stable levitation is impossible if the dust particle has a high initial velocity.

Based on the analysis above, it is clear that non-linearity in the system greatly enriches possible phenomena.

3.2 Dust transport across the terminator region

The terminator region is the area where space plasma and solar radiation change for both the lunar surface and the dust. Particles electrostatically released from the surface are more likely to move across the terminator region, where horizontal electric fields are much larger than in other regions on the dayside of the Moon (Figure 2b). Data also show that levitation status can also change greatly in the proximity of the terminator region, and that a range of dust phenomena can be expected.

In the first place, we examined effects in the dawn terminator region. In this case, a dust particle with r_d=0.05 μm, and Q_0=−17e was launched into the sheath before sunrise (sza=90.5°) at the equator (θ=90°, ϕ=−90.5°), and v_{z0}=0. Figure 7 shows its trajectory in the x-z plane, with colors indicating charge state. At first, this particle is in the dark, but its charge becomes more negative as it oscillates up to its stable levitation height around 200 m and moves eastward under the influence of the horizontal electric field. As the dust particle moves into sunlight, photoelectron emissions take control of the total charging current, and the particle charge becomes less negative. Examining the trajectory shown in Figure 7, it is clear that there is a dramatic change in oscillation that occurs when the particle moves to an sza of 90°, where the charging current, I, turns positive. Since the sheath potential is negative, on the basis of eq. (12), the system suddenly changes from energy gain to energy loss, and oscillation switches from amplified to damped. However, since no stable levitation is possible in the shaded region of Figure 5, the particle finally drops down into the regolith as expected. Overall, total transportation time was about 1 hour, and the dust particle has moved about 1000 m to the east.

Things are quite different if the dust particle is launched at dusk (θ=90°, ϕ=90.2°), because of solar radiation related to the rotation of the Moon. At dusk, the horizontal

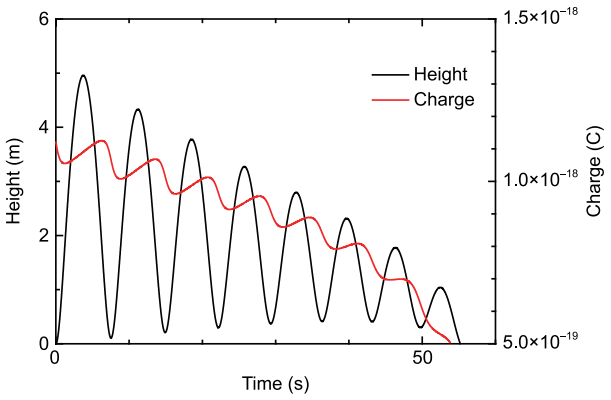

Figure 6 Unstable levitation, r_d=0.05 μm, v_{z0}=0, Q_0=7e, sza=0.

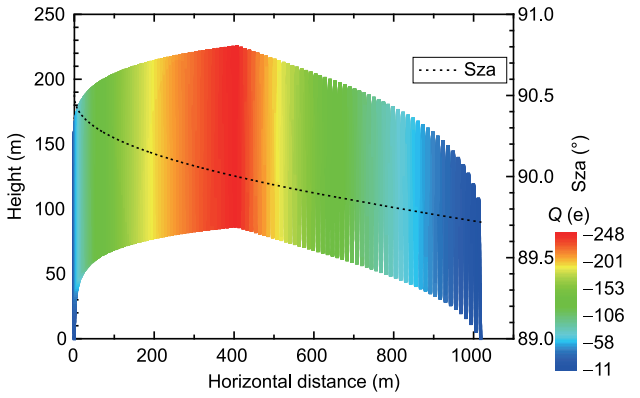

Figure 7 Dust transport in the dawn terminator region; r_d=0.05 μm, Q_0=−17e, v_{z0}=0.

electric field is eastward, and thus a negatively charged dust particle is doomed to move westward (Figure 8). However, since the Moon rotates in an eastward direction, the particle will remain longer in dark (sza>90°) than the case in the dawn terminator region. At first, as the dust does not gain high westward speed, the sza of its location gets higher as the Moon rotates, and it takes more than 5 hours for the particle to gain a horizontal speed large enough to cancel out this rotation. During this time, the particle becomes charged to a high negative equilibrium potential, but since the current is negative, it gains energy and oscillations are amplified until it passes into the sunlight. Subsequently, photoelectron emissions lead to a neutralization of negative charge, oscillation becomes damped, and trajectory height is lowered as a result of energy loss and negative charge. Eventually, transport stops when the particle drops to the ground, although horizontal displacement has been very long, up to 270 km over more than 140 hours (six Earth days).

4. Discussion and conclusions

According to plasma sheath theory and recent observations of the lunar plasma environment, we present a global near-surface plasma environment model. We solved equations of motion and charging for dust particles in the near-surface plasma environment, studied their dynamics, and discussed dust particle levitation conditions from the energy conservation point of view. We also simulated dust transportation near the terminator region.

Results of our modeling work show that in solar wind, the dayside Moon surface is usually positively charged to potentials in the magnitude of the lunar photoelectron energy (in eV), while the nightside surface is negatively charged to potentials in the magnitude of the plasma electron energy (in eV) in the lunar wake. The scale height of the dayside sheath is around 1 m, while the nightside has much thicker sheath with scale height up to kilometers. With different sheath profile, the dayside sheath of the Moon is usually dominated by a vertical electric field, while many regions on the nightside have both vertical and horizontal electric field components. However, globally speaking, the horizontal electric field component is usually more than three orders of magnitude weaker than the vertical component.

In the near-surface environment, dust particles of certain sizes can be levitated stably by the electric field. However, as the Moon is a celestial body with a relatively large gravity, dust particles that can be levitated are usually small, no larger than sub-micron scales. On the dayside of the Moon, these particles can be up to ten times smaller than these on the nightside. Stably levitated particles collect in a belt over the lunar surface; on the dayside of the Moon, this belt is less than 10 m thick, while on the nightside it can be up to 10 km thick. Between the lower boundary of this belt and the surface, there is also a layer where dust particles cannot be stably suspended on the dayside of the Moon. Although the size and charge of stably levitated particles are dependent only on local plasma conditions, both initial velocity and charge are important factors in determining whether, or not, a particle can finally reach equilibrium force and charge. Our results show that both a large initial velocity and charge are unfavorable if a dust particle is to reach stable levitation. However, on the other hand, too small an initial charge is also a disadvantage, as a particle either will be unable to overcome gravity, or will be unstably levitated.

Near to the terminator region, although the horizontal electric field is below several millivolt/m, its impact on dust particle dynamics is significant. Driven by the horizontal electrostatic force, negatively charged particles may move from the dark side of the Moon towards the sunlit hemisphere. During transport, a particle accumulates more negative charges

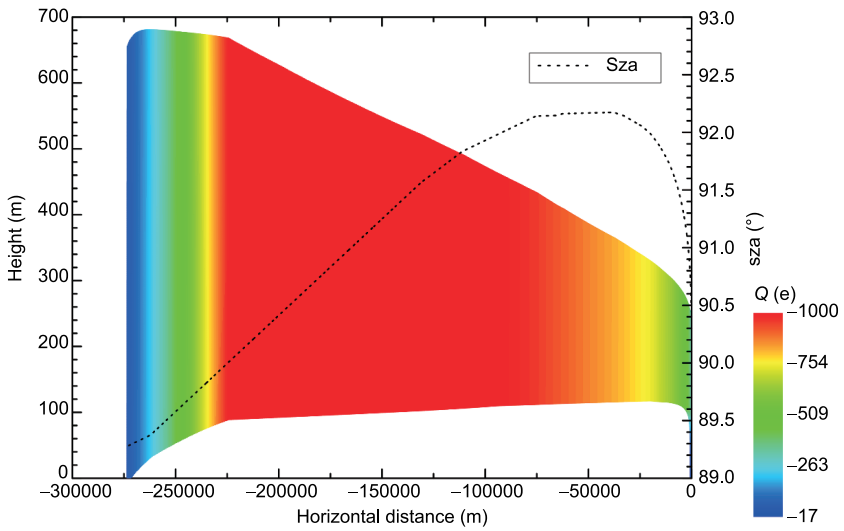

Figure 8 Dust transport in the dusk terminator region; r_d=0.05 μm, Q_0=−17e, v_{z0}=0.

and gains energy in the dark, leading to a higher trajectory and larger amplitude of oscillation; once in the sunlight, a particle begins to lose both negative charge and energy, resulting in a lowered trajectory and damped oscillation, before it finally falls to the ground. Although the sheath profiles are symmetric for both dawn and dusk, dust particle dynamics at the two times are quite different, because of the rotation of the Moon. At dawn, dust moves eastwards in the same direction as rotation, and comes into the sunlight before becoming too highly negatively charged. In contrast, at dusk, a particle moves in the anti-rotation direction, but because horizontal acceleration is weak, it usually takes tens of hours for its acceleration to counter rotation. At the same time, the particle develops a high negative charge and can even reach equilibrium. By the time a highly negatively charged particle races into the sunlight, it may have attained a very large amplitude of oscillation, which can last for several days before it crashes into the ground before sunset. Thus, the particle transport time is much longer if launched at sunset rather than at dawn, and simulation results suggest that the terminator region is the place where net deposition of dust from the dark hemisphere into the sunlit hemisphere takes place.

It is nevertheless worth noting that in this research, we have assumed that dust is so tenuous that the charge carried by particles does not affect the sheath plasma, and that there is no Coulomb interaction between dust particles. This assumption is likely fair on the Moon some of the time as the charge density on the lunar surface is 3×10^8 e/m^2; this means that just 1 grain out of every 100 can carry a charge (Poppe and Horányi, 2010). However, perturbations from human or robot activity, as well as meteoroid impacts can produce large amounts of charged dust. If this is the case, then the problem should be addressed by solving the Vlasov-Poisson system self-consistently using the Particle in Cell (PIC) method (Anuar et al., 2013). Due to our currently limited computational capabilities, however, PIC can only be applied to small-scale dust problems at present (Anuar, 2013).

In our work, we have extended current understanding of the dynamics of lunar dust from a simply dayside perspective to a global view. However, due to limited observations, there are still some uncertainties about the plasma environment in the lunar wake which might give rise to uncertainties in sheath and dust charging on the nightside of the Moon. On the other hand, electron temperatures inside the wake can exceed 100 eV, secondary electron yield may play a role in influencing the equilibrium electric potential both of the lunar surface and dust particles (Nitter et al., 1998).

In summary, this study shows that the problem of lunar dust is both highly non-linear and manifested in a variety of ways. Additional theoretical studies, as well as measurements of the plasma environment and dust mobility on the lunar surface, are needed to fully understand the charging and motion of dust particles on the Moon.

Acknowledgements *This work was supported by the National Natural Science Foundation of China (Grant No. 41174115).*

References

Anuar A K. 2013. A study of dusty plasma environment. Doctoral Dissertation. Lancashire: Lancaster University

Anuar A K, Honary F, Hapgood M, Roussel J F. 2013. Three-dimensional simulation of dust charging and dusty plasma using SPIS. J Geophys Res Space Phys, 118: 6723–6735

Berg O E, Wolf H, Rhee J. 1976. Lunar soil movement registered by the Apollo 17 cosmic dust experiment. In: Elsässer H, Fechtig H, eds. Interplanetary Dust and Zodiacal Light. New York: Springer-Verlag. 233–237

Colwell J E, Batiste S, Horányi M, Robertson S, Sture S. 2007. Lunar surface: Dust dynamics and regolith mechanics. Rev Geophys, 45: RG2006

Colwell J, Gulbis A, Horanyi M, Robertson S. 2005. Dust transport in photoelectron layers and the formation of dust ponds on Eros. Icarus, 175: 159–169

Freeman J W, Ibrahim M. 1975. Lunar electric fields, surface potential and associated plasma sheaths. The Moon, 14: 103–114

Guernsey R L, Fu J H M. 1970. Potential distribution surrounding a photoemitting, plate in a dilute plasma. J Geophys Res, 75: 3193–3199

Halekas J S, Bale S D, Mitchell D L, Lin R P. 2005. Electrons and magnetic fields in the lunar plasma wake. J Geophys Res, 110: A07222

Manka R H. 1973. Plasma and potential at the lunar surface. In: Grad, eds. Photon and Particle Interaction with Surfaces in Space. Dordrecht-Holland: DReidel Publishing Company. 347–361

Nishino M N, Maezawa K, Fujimoto M, Saito Y, Yokota S, Asamura K, Tanaka T, Tsunakawa H, Matsushima M, Takahashi F, Terasawa T, Shibuya H, Shimizu H. 2009a. Pairwise energy gain-loss feature of solar wind protons in the near-Moon wake. Geophys Res Lett, 36: L12108

Nishino M N, Fujimoto M, Maezawa K, Saito Y, Yokota S, Asamura K, Tanaka T, Tsunakawa H, Matsushima M, Takahashi F, Terasawa T, Shibuya H, Shimizu H. 2009b. Solar-wind proton access deep into the near-Moon wake. Geophys Res Lett, 36: L16103

Nitter T, Havnes O, Melandsø F. 1998. Levitation and dynamics of charged dust in the photoelectron sheath above surfaces in space. J Geophys Res, 103: 6605–6620

Nitter T, Aslaksen T K, Melandso F, Havnes O. 1994. Levitation and dynamics of a collection of dust particles in a fully ionized plasma sheath. IEEE Trans Plasma Sci, 22: 159–172

Nitter T, Havnes O. 1992. Dynamics of dust in a plasma sheath and injection of dust into the plasma sheath above Moon and asteroidal surfaces. Earth Moon Planet, 56: 7–34

Poppe A, Horányi M. 2010. Simulations of the photoelectron sheath and dust levitation on the lunar surface. J Geophys Res, 115: A08106

Rennilson J J, Criswell D R. 1974. Surveyor observations of lunar horizon-glow. Earth Moon Planets, 10: 121–142

Whipple E C. 1981. Potentials of surfaces in space. Rep Prog Phys, 44: 1197–1250

Willis , R F, Anderegg M, Feuerbacher B, Fitton B. 1973. Photoemission and secondary electron emission from lunar surface material. In: Gerard R J L, eds. Photon and Particle Interactions with Surfaces in Space. New York: Springer. 369–387

Zook H A, Potter A E, Cooper B L. 1995. The lunar dust exosphere and Clementine lunar horizon glow. Lunar Planet Sci, 26: 1577–1578